ACS APPLIED MATERIALS & INTERFACES

Research Article

www.acsami.org

Surface Modification of Siliceous Materials Using Maleimidation and Various Functional Polymers Synthesized by Reversible Addition–Fragmentation Chain Transfer Polymerization

Hirokazu Seto,[†] Masaki Takara,[†] Chie Yamashita,[†] Tatsuya Murakami,[‡] Takeshi Hasegawa,[§] Yu Hoshino,[†] and Yoshiko Miura*,[†]

[†]Department of Chemical Engineering, Graduate School of Engineering, Kyushu University, 744 Motooka, Nishi-ku, Fukuoka 819-0395, Japan

[‡]Center for Nano Materials and Technology, Japan Advanced Institute of Science and Technology, 1-1 Asahidai, Nomi, Ishikawa 923-1292, Japan

[§] Laboratory of Solution and Interface Chemistry, Division of Environmental Chemistry, Institute for Chemical Research, Kyoto University, Uji, Kyoto 611-0011, Japan

Supporting Information

ABSTRACT: A novel surface modification method was investigated. The surface of siliceous materials was modified using polystyrene, poly(acrylic acid), poly(*N*-isopropylacrylamide), and poly(*p*-acrylamidophenyl-α-mannoside) synthesized by reversible addition–fragmentation chain transfer polymerization. Thiol-terminated polymers were obtained by reduction of the thiocarbonate group using sodium borohydride. The polymers were immobilized on the surface via the thiol–ene click reaction, known as the Michael addition reaction. Immobilization of the polymers on the maleimidated surface was confirmed by X-ray photoelectron spectroscopy, infrared spectroscopy, and contact angle measurements. The polymer-immobilized surfaces were observed by atomic force microscopy, and the thickness of the polymer layers was determined by ellipsometry. The thickness of the polymer immobilized by the maleimide–thiol reaction was less than that formed by spin coating, except for polystyrene. Moreover, the polymer-immobilized surfaces were relatively smooth with a roughness of less than 1 nm. The amounts of amine, maleimide, and polymer immobilized on the surface were determined by quartz crystal microbalance measurements. The area occupied by the amine-containing silane coupling reagent was significantly less than the theoretical value, suggesting that a multilayer of the silane coupling reagent was formed on the surface. The polymer with low molecular weight had the tendency to efficiently immobilize on the maleimidated surface. When poly(*p*-acrylamidophenyl-α-mannoside)-immobilized surfaces were used as a platform for protein microarrays, strong interactions were detected with the mannose-binding lectin concanavalin A. The specificity of poly(*p*-acrylamidophenyl-α-mannoside)-immobilized surfaces for concanavalin A was compared with poly-L-lysine-coated surfaces. The poly-L-lysine-coated surfaces nonspecifically adsorbed both concanavalin A and bovine serum albumin, while the poly(*p*-acrylamidophenyl-α-mannoside)-immobilized surface preferentially adsorbed concanavalin A. Moreover, the poly(*p*-acrylamidophenyl-α-mannoside)-immobilized surface was applied to micropatterning with photolithography. When the micropattern was formed on the poly(*p*-acrylamidophenyl-α-mannoside)-spin-coated surface by irradiation with ultraviolet light, the pattern of the masking design was not observed on the surface adsorbed with fluorophore-labeled concanavalin A using a fluorescent microscope because of elution of poly(*p*-acrylamidophenyl-α-mannoside) from the surface. In contrast, fluorophore-labeled concanavalin A was only adsorbed on the shaded region of the poly(*p*-acrylamidophenyl-α-mannoside)-immobilized surface, resulting in a distinctive fluorescent pattern. The surface modification method using maleimidation and reversible addition–fragmentation chain transfer polymerization can be used for preparing platforms for microarrays and micropatterning of proteins.

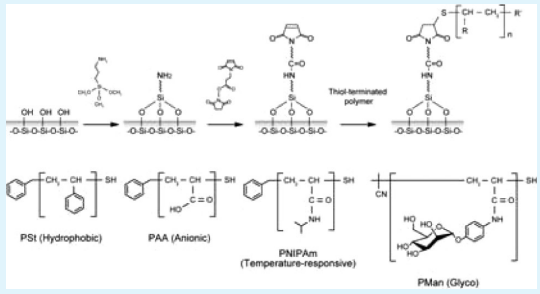

KEYWORDS: *surface modification, RAFT polymerization, maleimide, thiol, microarray*

1. INTRODUCTION

Surface modification with polymers is an effective method for preparing materials with the functionality of the polymer. To obtain polymer functional surfaces, control of the polymer density and their orientation on the surface is important.

Received: February 27, 2012
Accepted: September 26, 2012
Published: September 26, 2012

dx.doi.org/10.1021/am301637q | *ACS Appl. Mater. Interfaces* 2012, 4, 5125–5133

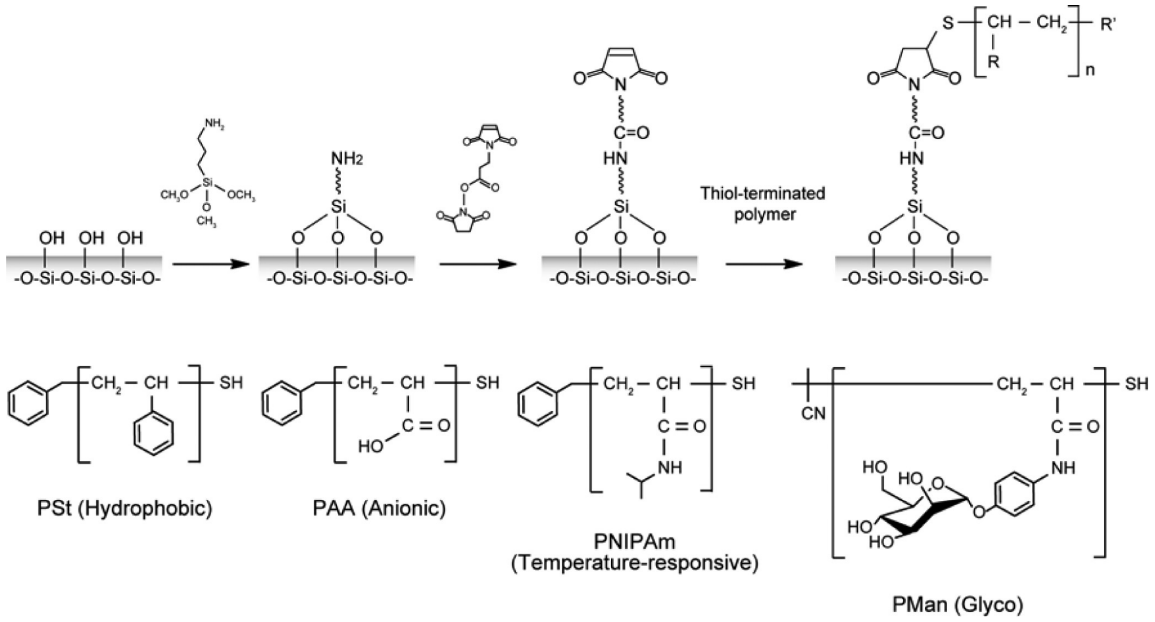

Figure 1. Preparation of maleimidated surface and immobilization of thiol-terminated polymer via the Michael addition reaction.

Therefore, the polymer needs to be easily, strongly, uniformly, and thinly immobilized on the surface. In addition, the techniques need to be applicable to a wide variety of materials such as metals, silica, plastics, and cellulose.

Reversible addition−fragmentation chain transfer (RAFT) polymerization is a technique for the precise synthesis of polymers with low polydispersity.[1−3] RAFT polymerization is similar to conventional free-radical polymerization, except for the addition of a chain transfer agent which includes a thiocarbonylthio compound. Polymers obtained by RAFT polymerization retain the thiocarbonylthio group at the chain terminal. It is well-known that the polymers can be converted into thiol-terminated polymers by reduction.[4] The thiol group acts as a convenient binder between the surface and the polymer.

The interaction between gold (or other precious metals) and thiol groups is effective for self-assembly,[5,6] because of strong and rapid formation according to the hard and soft acids and bases rule,[7] and is useful for the preparation of biomaterials.[8,9] Thiol-terminated polymers synthesized by RAFT polymerization have also been immobilized on gold surfaces.[10−12] The polymers can be used to prepare biomaterials such as platforms for microarray and micropatterning of biomolecules by immobilization on surfaces other than gold. Covalent bonds between the thiol and N-substituted maleimide groups selectively and rapidly form via the thiol−ene click reaction, which is known as the Michael addition reaction.[13] Maleimidation of surfaces has been reported for functionalization with thiol compounds.[14−16]

Here, we describe surface modification using a combination of maleimidation and RAFT polymerization (Figure 1). The main aim of this study was to establish a novel strategy for the immobilization of polymers synthesized by RAFT polymerization onto siliceous surfaces. To demonstrate that the technique is applicable to a wide variety of polymers with different properties, polystyrene (PSt, hydrophobic polymer), poly(acrylic acid) (PAA, anionic polymer), poly(*N*-isopropylacrylamide) (PNIPAm, temperature-responsive polymer), and poly(*p*-acrylamidophenyl-*α*-mannoside) (PMan, glycopolymer) were used for immobilization on a silicon wafer, glass slide, and silica-sputtered oscillator. In addition, the glycopolymer-immobilized surface was applied to biomaterials, such as platforms for protein microarrays and micropatterning by photolithography.

2. EXPERIMENTAL SECTION

2.1. Reagents and Matrices. The following reagents were used as received: styrene (Kanto Chemical Co., Inc., Tokyo Japan), *tert*-butyl acrylate (*t*BAA, Tokyo Chemical Industry Co. Ltd., Tokyo, Japan), *N*-isopropylacrylamide (Wako Pure Chemical Industries Ltd., Osaka, Japan), D-mannose (Towa Chemical Industry Co. Ltd., Tokyo, Japan), 2,2′-azobisisobutyronitrile (AIBN, Wako Pure Chemical Industries Ltd., Osaka, Japan), 4,4′-azobis-4-cyanovaleric acid (V501, Sigma Co., St. Louis, MO, USA), 3-aminopropyl trimethoxysilane (APTMS, Azmax Co., Chiba, Japan), *N*-succinimidyl 3-maleimidopropionate (SMP, Tokyo Chemical Industry Co. Ltd., Tokyo, Japan), albumin from bovine serum (BSA, Sigma Co., St. Louis, MO, USA), concanavalin A (Con A, J-Oil Mills Inc., Tokyo, Japan), and FITC-Con A (Seikagaku Biobusiness Corporation, Tokyo, Japan). Fluorescein isothiocyanate isomer (FITC-I, Dojindo Laboratories, Kumamoto, Japan) was used for synthesis of FITC-BSA. A silicon wafer, glass slide, and silica-sputtered oscillator (effective surface area: 4.9 mm^2, Initium Inc., Tokyo, Japan) were used as the matrix.

2.2. Preparation of Thiol-Terminated Polymers via RAFT Polymerization. Thiol-terminated polymers were prepared by synthesis of trithiocarbonate-terminated polymer via RAFT polymerization and conversion of the trithiocarbonate group into the thiol group by $NaBH_4$ reduction. The detailed processes for the preparation of the thiol-terminated polymers are described in the Supporting Information (Figures S1−S7). Polymer molecular weights were determined using size exclusion chromatography with the chromatograph connected to a Shodex LF804 column (Showa Denko KK., Kanagawa, Japan), using dimethylformamide with LiBr (10 mmol/L) as the mobile phase.

2.3. Preparation of Thiol-Terminated Polymer-Immobilized Surfaces. The surfaces of a silicon wafer and glass slide were washed by sonication in acetone, ethanol, and Milli-Q water (Millipore Corporation, Billerica, MA, USA). After UV/O_3 treatment for 30 min, the surfaces were activated in RCA solution (water:hydrogen peroxide:ammonia = 5:1:1) at 60 °C for 20 min. The matrices were immersed in APTMS aqueous solution (1 vol %) at 60 °C for 3 h and then at 110 °C for 5 min. After the surfaces were washed with water,

the aminated matrices were immersed in SMP solution (DMSO, 1.5 mmol/L) and then incubated in the dark at room temperature for 6 h. The surfaces were then washed with DMSO. The maleimidated matrices were immersed in the thiol-terminated polymer solution (Milli-Q water or DMSO, 1.0 g/L) and then incubated in the dark at room temperature for 12 h. DMSO solvent was used for immobilization of PSt due to water insolubility of the hydrophobic polymer. The thiol-terminated polymer-immobilized surfaces were obtained by washing with water or DMSO and drying.

The surface of the oscillator in the quartz crystal microbalance (QCM) cell was activated with a drop of piranha solution (sulfuric acid:hydrogen peroxide = 3:1, 5 μL), instead of UV/O_3 and RCA treatments. The cell holder was filled with APTMS solution and incubated at 60 °C for 3 h and then at 110 °C for 5 min. After the surface was washed with water, SMP solution was added dropwise onto the oscillator, and then the surface was incubated in the dark at room temperature for 6 h. The surfaces were then washed with DMSO/water (50:50). Thiol-terminated polymer solution was added dropwise onto the oscillator, and then the surface was incubated in the dark at room temperature for 12 h. The thiol-terminated polymer-immobilized oscillator was obtained by washing with water or DMSO/water (50:50) and drying.

Polymer layers were also formed by spin coating for comparison. The polymer solutions (50 μL) were prepared at the same concentration (1.0 g/L) with immobilization of the polymer by the maleimide−thiol reaction. The polymer solution was dropped onto the silicon wafer or glass slide (1 cm × 1 cm), followed by high-speed spinning at 3000 rpm using a spin coater (Opticoat MS-A100, Mikasa Co, Ltd., Tokyo, Japan). After spinning for 30 s, the silicon wafer and glass slide were treated by heating at 110°C.

2.4. Characterization of Thiol-Terminated Polymer-Immobilized Surfaces. To confirm amination, maleimidation, and polymer immobilization on the surfaces, the surface properties were evaluated by X-ray photoelectron spectroscopy (XPS), infrared (IR) spectroscopy, atomic force microscopy (AFM), ellipsometry, and contact angle measurements using a silicon wafer. The existence of functional groups and polymers on the silicon wafer was confirmed by C(1s), N(1s), and S(2p) XPS (AXIS-ultra, Shimadzu/Kratos, Kyoto, Japan). The obtained XPS spectra were peak-divided by Peak Fit software. The IR spectra of the surface adsorbates on a silicon wafer were obtained using an FT-IR spectrometer (Magna 550, Thermo Fisher Scientific, Madison, USA) with the external-reflection (ER) optical configuration employing *p*-polarization. A reflection attachment (RMA-1DG/VRA, Harrick Scientific Products Inc., Ossining, USA) was used to perform the ER measurements with an angle of incidence of 60°. A liquid-N_2-cooled MCT (Hg−Cd−Te) detector was used, and the modulation frequency was 60 kHz. The wavenumber resolution was 4 cm^{-1}, and the accumulation number was 2000. The *p*-polarized IR ray was generated by a wire-grid polarizer (PWG-U1R, Harrick Scientific Products Inc.). For the IR-ER measurements, the samples were prepared on a single-side polished Si wafer, which allows the surface selection rule of ER spectrometry[17] to be taken into account.

The surface topography of the thiol-terminated polymer-immobilized silicon wafer was determined by AFM (Dimension Icon AFM, Bruker AXS, Karlsruhe, Germany) using tapping mode with an antimony-doped Si probe (spring constant: 20−80 N/m, NCHV-10, Bruker AXS K.K., Yokohama, Japan) in air. The AFM images were captured in a 500 μm × 500 μm area. Image analysis and roughness measurements were performed with NanoScope Analysis software. The thickness of the polymer immobilized on the surface was determined by an imaging ellipsometer (NL-MIE, Nippon Laser & Electronics Lab., Nagoya, Japan) using a 532 nm YAG laser in air. The reflective index of poly(*N*-phenylacrylamide) was used as a substitute for that of PMan. The contact angle on the silicon wafers was measured by the sessile drop method (DropMaster 300, Kyowa Interface Science, Saitama, Japan) at 26 °C. The contact angle of the water droplet on the PAA-immobilized silicon wafer was determined after treatment with HCl/KCl buffer (pH 2.0). The contact angle on the PNIPAm-immobilized silicon wafer was also determined after heating at 60 °C. All measurements were performed at five spots on the surfaces.

2.5. Determination of Amount of Amine, Maleimide, and Thiol-Terminated Polymer Immobilized Using QCM. The amounts of amine, maleimide, and thiol-terminated polymer immobilized on the oscillator in the QCM cell were determined by QCM measurements (AFFINIXQ4, Initium Inc., Tokyo, Japan). The frequencies after amination, maleimidation, and polymer immobilization were monitored at a dry state. The amounts of the functional group and polymer immobilized were estimated from the difference of the frequency with the previous step. The relationship between the frequency change (ΔF, Hz) and the adsorbed mass (Δm, ng/cm^2) was defined by the Sauerbrey equation[18]

$$\Delta F = -\frac{2NF_0^2}{\sqrt{\rho\mu}}\Delta m \quad (1)$$

where N, F_0, ρ, and μ are the harmonic overtone, the fundamental resonance frequency, the crystal density, and the elastic modulus of the crystal, respectively. The F_0 of the apparatus used was 27 MHz. Thus, eq 1 can be simplified as

$$\Delta m \cong -0.62 \times \Delta F \quad (2)$$

2.6. Fluorescent Measurements of Proteins Adsorbed on a Thiol-Terminated Polymer-Immobilized Glass Slide. The fluorescence intensities on the PMan-immobilized surface were determined using FITC-labeled proteins. Con A is a mannose-binding lectin. Silicon rubber wells (diameter: 3 mm) were attached to the PMan-immobilized and the PMan-spin-coated glass slides, and then various concentrations of FITC−BSA and FITC−Con A solutions in phosphate-buffered saline (pH: 7.4, 5 μL) were added into the wells. After incubation in the dark for 2 h and washing with water, the surfaces adsorbed with FITC proteins were observed with a fluorescent microscope (BZ-8000, Keyence Corporation, Osaka, Japan). The relative intensity (I/I_0) on the surface was estimated from the gray value obtained by ImageJ software.

Detection of protein on the PMan-immobilized glass slide was compared with that on the commercially available glass slide. A poly-L-lysine-coated glass slide (25.4 mm × 76.2 mm, Matsunami Glass Ind., Ltd., Osaka, Japan) was used as a commercially available platform of microarray. Various concentrations of FITC−BSA and FITC−Con A solutions were added into the wells on the PMan-immobilized and poly-L-lysine-coated glass slides. After incubation in the dark for 2 h and washing with water, the microarray spots on the PMan-immobilized and poly-L-lysine-coated glass slides were scanned by a microarray scanner (FLA-8000, Fujifilm Corporation, Tokyo, Japan) at 532 nm.

The PMan-immobilized glass slide was prepared by the photolithographic technique. The PMan-immobilized and PMan-spin-coated glass slides were micropatterned by exposure to UV light at 254−365 nm and 10 mW/cm^2 using a high-power xenon light source (MAX-302, Asahi Spectra Co., Ltd., Tokyo, Japan) through a Cu-microgrid mesh with a diameter of ca. 3000 μm, a thickness of 25 μm, and a pitch width of 150 μm (Okenshoji Co., Ltd., Tokyo, Japan) for 24 h. The micropatterned glass slide was immersed in FITC−Con A solution (10 mg/L). After incubation in the dark for 2 h and washing with a sufficient quantity of water, the micropatterned surface was observed by fluorescent microscopy. The gray value on the surface was linearly scanned by ImageJ software to determine the geometry of the patterning.

3. RESULTS AND DISCUSSION

3.1. Physical Properties of Polymers Synthesized by RAFT Polymerization. PSt, P*t*BAA, PNIPAm, and PAcMan with trithiocarbonate termini were synthesized by RAFT polymerization. P*t*BAA and PAcMan were used as protecting precursors for PAA and PMan, respectively. The molecular weight of the trithiocarbonate-terminated polymer was determined by size exclusion chromatography (Figure 2).

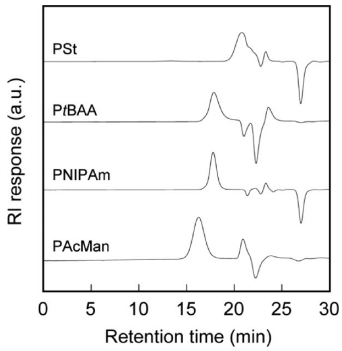

Figure 2. Size exclusion chromatograms of PSt, P*t*BAA, PNIPAm, and PAcMan synthesized by RAFT polymerization.

The weight-average molecular weight (M_w), the number-average molecular weight (M_n), and the polydispersity (M_w/M_n) for the trithiocarbonate-terminated polymers are listed in Table 1. The M_w/M_n values for PSt, P*t*BAA, PNIPAm, and PAcMan synthesized by RAFT polymerization were 1.18, 1.14, 1.06, and 1.14, respectively.

Table 1. Characteristics of the Polymers Synthesized by RAFT Polymerization

polymer	M_w[a]	M_n[a]	M_w/M_n
PSt	5130[b]	4350[b]	1.18[b]
P*t*BAA	28300	24900	1.14
PNIPAm	28900	27200	1.06
PAcMan	77000	67500	1.14

[a]The molecular weights were determined by size exclusion chromatography. PSt standards were used for preparation of the calibration curve. The calibration curve used was $\log M = -0.258t + 9.07$, where t is retention time. [b]The peak corresponding to PSt was overlapped with a ghost peak. The values of M_w, M_n, and M_w/M_n were 5400, 4750, and 1.14, respectively, after the peak was divided by Peak Fitting software.

3.2. Confirmation of Amination, Maleimidation, and Polymer Immobilization. The existence of amine groups, maleimide groups, and the polymers on the silicon wafer was confirmed by XPS (Figure 3). In the C(1s) and N(1s) spectra of the aminated surface, high-intensity peaks corresponding to C−C bonds (285.0 eV) and N−C and $-NH_2$ bonds (399.2 eV) were observed. In addition, the peak at 401.5 eV corresponds to hydrogen-bonded amine and positively charged amine.[19,20] The peak for the N−C bond of amide was observed at 400.2 eV in the N(1s) spectra of the maleimidated surface, confirming the presence of the amine and maleimide groups. The trimethoxysilyl group in the silane coupling reagent is covalently bonded to the hydroxyl groups of the silica glass,[20−28] metal oxides,[29−33] and cellulose.[24,34−37] Therefore, maleimidated surfaces can be prepared using various matrices, assuming that the polymers synthesized by RAFT polymerization can be immobilized on the matrix surfaces. In the C(1s) and N(1s) spectra of the thiol-terminated polymer-immobilized surfaces, the intensity of the peak corresponding to the C═O bond was observed at 288.1 eV, except for the PSt-immobilized surfaces. Because PSt does not have C═O, N−H, and N−C bonds in the chain, the intensities of the peaks corresponding to the C═O, N−H, and N−C bonds on the PSt-immobilized surface were weaker than those on the maleimidated surface, indicating that the silicon surface was mostly covered by PSt. The immobilization of polymers on the surface was also evaluated by the existence of sulfur atoms using XPS. No peaks were observed in the S(2p) XPS spectra of the aminated and maleimidated surfaces. In contrast, the peaks were observed for the polymer-immobilized surfaces, suggesting that the peaks correspond to thioether formed between the thiol group at the polymer chain terminal and the maleimide group on the surface. Therefore, it was confirmed that the thiol-terminated polymers could be immobilized on the maleimidated surface.

The existence and orientations of the amine groups, maleimide groups, and the polymers on the silicon wafer were determined by IR spectroscopy. The IR-ER spectra of the aminated, maleimidated, and polymer-immobilized surfaces are shown in Figure 4. In all of the spectra, the symmetric and antisymmetric CH_2 stretching vibration bands positively appeared at 2853 and 2931 cm^{-1}, respectively. The surface selection rule of *p*-polarized ER spectrometry is that a surface-parallel transition moment appears as a negative band, whereas a surface-normal transition moment gives a positive band when the angle of incidence (60°) is smaller than Brewster's angle (73° for the air/Si interface). This selection rule, however, only holds for the CH_2 stretching vibration bands when the hydrocarbon chain has an all-trans zigzag conformation. In the present results, the position of the bands at 2853 and 2931 cm^{-1} indicates that the hydrocarbon chain is disordered, which results in a tilted orientation for both modes on average. In other words, the molecules are loosely available on the Si surface. In this situation, the orientation is not significantly reflected in the band intensity and sign, and only the adsorbed quantity can be approximated. In Figure 4, the band intensities are found to increase after immobilization of the polymer, which can be attributed to the existence of main chains in the polymers. Nevertheless, it is estimated that the polymer was immobilized on the surface in a random manner, due to the low molecular density. The weak band intensity is not only due to the low molecular density but also to the random orientation. When the hydrocarbon chains have a perpendicular arrangement to the surface, which is commonly found in alkylic self-assembled monolayers and Langmuir−Blodgett films, the band intensity becomes much stronger, and the sign becomes negative. Focusing on the spectral region around 1700 cm^{-1} of the PAA-, PNIPAm-, and PMan-immobilized surfaces, the C═O stretching vibration mode appears as a broad band (Figure S8, Supporting Information) indicating various types of hydrogen bonds. Molecular interactions via the amide groups have thus been confirmed. The weak peak between 1600 and 1800 cm^{-1} in the spectra of the PSt-immobilized surface can be attributed to the C═C stretching vibration mode in the aromatic ring. Therefore, the IR-ER spectra indicate that the quantity of introduced chains is not high, but they are definitely immobilized.

The contact angle of water droplets on the silicon wafers was measured by the sessile drop method (Figure 5). The contact angle on the unmodified silicon wafer indicated that it was hydrophilic (Figure 5a, 21.1°). When the amine and maleimide groups were immobilized on the silicon wafer, the contact angles increased (Figure 5b and c, 69.0° and 57.0°, respectively). Chauhan et al. have formed APTMS multilayers on SiO_x/Si substrates via the silane coupling reaction and investigated the relationship between the number of APTMS layers (thickness) and the preparation conditions.[38] According to their results, the contact angles on the aminated surface increased with increasing number of APTMS layers, where the

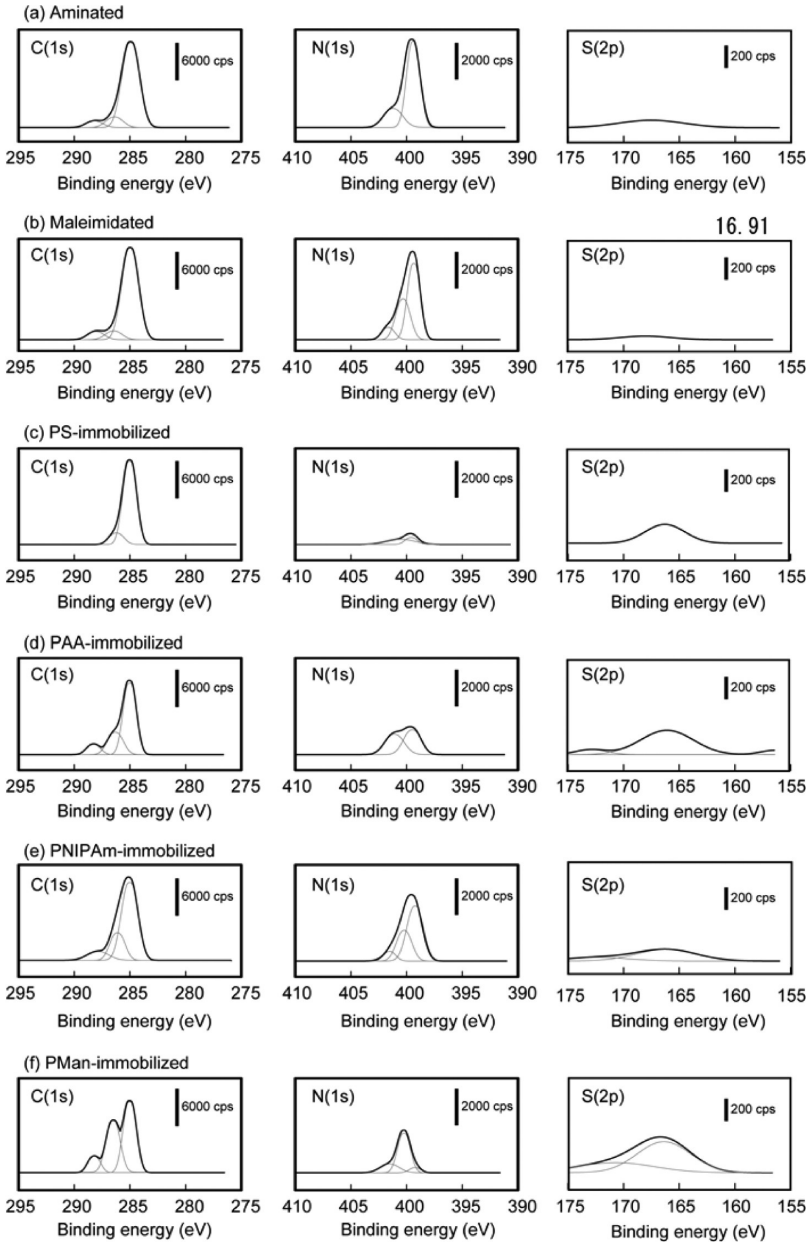

Figure 3. XPS spectra of (a) aminated, (b) maleimidated, (c) PSt-immobilized, (d) PAA-immobilized, (e) PNIPAm-immobilized, and (f) PMan-immobilized silicon wafers, prepared by the maleimide-RAFT process. The peak corresponding to C−C at 285.0 eV in the C(1s) spectrum was used for calibration. The weak peak observed at 288.3 eV in the C(1s) spectra of the unmodified and aminated surfaces could be due to carbon atoms of residual dust.

contact angle on the surface with ten APTMS layers was 40°. Therefore, in our study, APTMS was also immobilized on the surface as a multilayer because of the longer incubation times and the higher APTMS concentrations than the conditions used by Chauhan et al. The contact angles depend on the hydrophilicity/hydrophobicity of the immobilized polymer. The PSt-, PAA-, PNIPAm-, and PMan-immobilized surfaces had contact angles of 83.0°, 41.5°, 52.3°, and 35.4°, respectively, at room temperature. The PAA-immobilized silicon wafer was treated with HCl/KCl buffer (pH 2.0). The contact angle on the PAA-immobilized silicon wafer slightly increased after treatment (Figure 5f, 51.9°). The pK_a of PAA is approximately 4.5.[39] Because PAA on the surface is protonated at pH 2, the PAA-immobilized surface becomes hydrophobic. The contact angle on the PNIPAm-immobilized silicon wafer was also determined after heating at 60 °C. The PNIPAm-immobilized surface, which showed hydrophilic behavior at 26 °C (Figure 5g, 52.3°), became hydrophobic upon heating (Figure 5h, 66.7°). This indicates that the hydrophilicity/hydrophobicity of the PNIPAm-immobilized surface can be switched by temperature. The contact angle on the PMan-immobilized surface was relatively low, owing to the hydrophilic saccharide moiety in the polymer (Figure 5i, 35.4°). Surface modification by the maleimidation-RAFT process was achieved using polymers with different properties.

3.3. Observation of Polymer-Immobilized Surface. The morphology of the polymer layer surfaces was determined by AFM (Figure 6). In addition, the roughness and thickness of the polymers on the surface prepared by spin coating and the maleimide-RAFT process are listed in Table 2. All of the

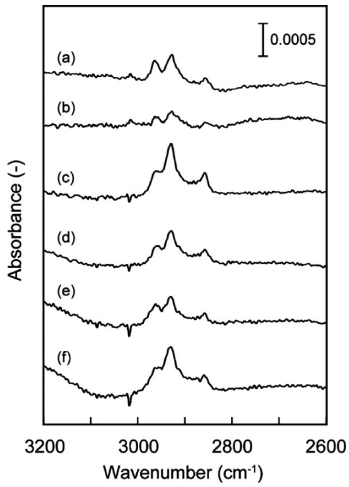

Figure 4. IR-ER spectra of (a) aminated, (b) maleimidated, (c) PSt-immobilized, (d) PAA-immobilized, (e) PNIPAm-immobilized, and (f) PMan-immobilized silicon wafers, prepared by the maleimide-RAFT process.

polymer-immobilized surfaces prepared by spin coating were flat, with a root mean-square (RMS) roughness of less than 0.3 nm. The ellipsometric thicknesses of the polymer layers formed by spin coating were in the order of PSt < PAA ≅ PNIPAm < PMan, which corresponds to the molecular weights of the polymers.

The polymer-immobilized surfaces formed by the maleimide-RAFT process were rough, compared with those formed by spin coating. Nevertheless, the RMS roughnesses of the polymer-immobilized surfaces obtained by the maleimide-RAFT process were less than 1 nm. The low roughness of each surface is probably due to low polydispersity of the polymer synthesized by RAFT polymerization. The amine group catalyzes condensation between the silane coupling reagent as well as formation of the siloxane bonds to the surface.[40] The ellipsometric thickness of the amine layer was ca. 2 nm. Because the theoretical length of the APTMS molecule is 0.7 nm,[38] APTMS was immobilized on the surface as a multilayer. The thickness after maleimidation was not significantly greater than after amination. The thickness of the polymer layer by the maleimide-RAFT process was calculated by subtracting the thickness after maleimidation from that after polymer immobilization. Apart from the PSt-immobilized surfaces, the polymer-immobilized surfaces formed by the maleimide-RAFT process were thinner than those formed by spin coating. PSt has lower molecular weights than the other thiol-terminated polymers (Table 1). The accessibility of the polymer onto the surface is strongly influenced by steric hindrance, suggesting that PSt efficiently reacted with the maleimide group on the surface. The polymer immobilization technique using the maleimide-RAFT process enables the formation of relatively smooth and thin polymer layers.

3.4. Amount of Amine, Maleimide, and Immobilized Polymers. The amounts of amine, maleimide, and immobilized polymer were estimated from ΔF in the drying state and are shown in Table 3. The area occupied by the normally oriented silanetriol has been reported to be 0.24 nm^2/molecule.[41] The amount of immobilized APTMS in Table 3 represents 0.0051 nm^2/molecule, suggesting that APTMS was immobilized on the surface in the form of a multilayer. The amount of the maleimide group on the surface was less than that of the amine group, indicating that SMP was preferentially bound with just the amine group at the top layer of the APTMS. A larger amount of PSt was immobilized on the surface than the other thiol-terminated polymers, which can be attributed to PSt being the smallest polymer and having the highest accessibility to the maleimidated surface. The large amount of immobilized PSt is in agreement with the ellipsometric results, which indicated that the PSt layer was thicker than the other polymer layers. The amounts of the other polymers were in the same range.

3.5. Microarray of Proteins Using Thiol-Terminated Polymer-Immobilized Glass Slides. The PMan-immobilized surfaces were viewed with a fluorescence microscope after adsorption of FITC proteins. The I/I_0 plots of the FITC proteins on the PMan-immobilized glass slides prepared by spin coating and the maleimide-RAFT process are shown in Figure 7. The I/I_0 values for both FITC proteins increased above 10^{-3} g/L. FITC−Con A was more adsorbed on the PMan-immobilized surfaces than FITC−BSA because of the specificity between Con A and Man. The I/I_0 of Con A on the PMan-spin-coated glass slide was less than that on the PMan-immobilized glass slide. Since spin-coated PMan is not covalently bonded to the surface, the PMan is eluted from the surface during incubation in protein solution.

The protein-recognition ability of the PMan-immobilized glass slide was compared with a commercially available (poly-L-lysine-coated) glass slide (Figure 8). On the poly-L-lysine-coated glass slide, both spots for FITC−Con A and BSA were observed at 0.05 g/L. In contrast, the spots for FITC−Con A

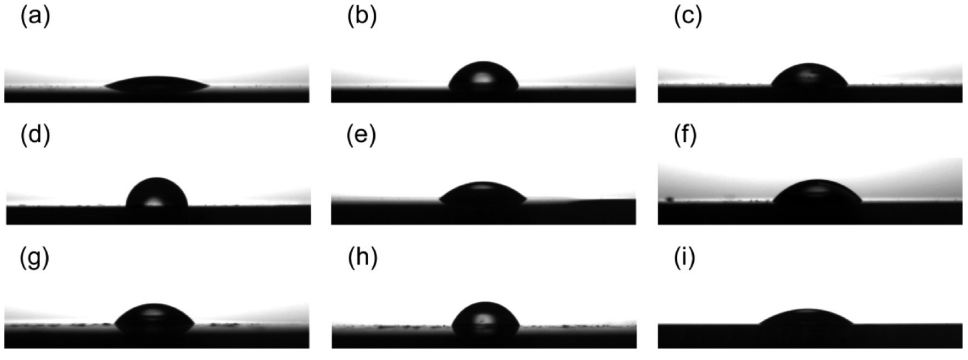

Figure 5. Images of a water droplet on (a) unmodified, (b) aminated, (c) maleimidated, (d) PSt-immobilized, (e) PAA-immobilized (before treatment at pH 2), (f) PAA-immobilized (after treatment at pH 2), (g) PNIPAm-immobilized (before heating), (h) PNIPAm-immobilized (after heating at 60°C), and (i) PMan-immobilized silicon wafers, prepared by the maleimide-RAFT process.

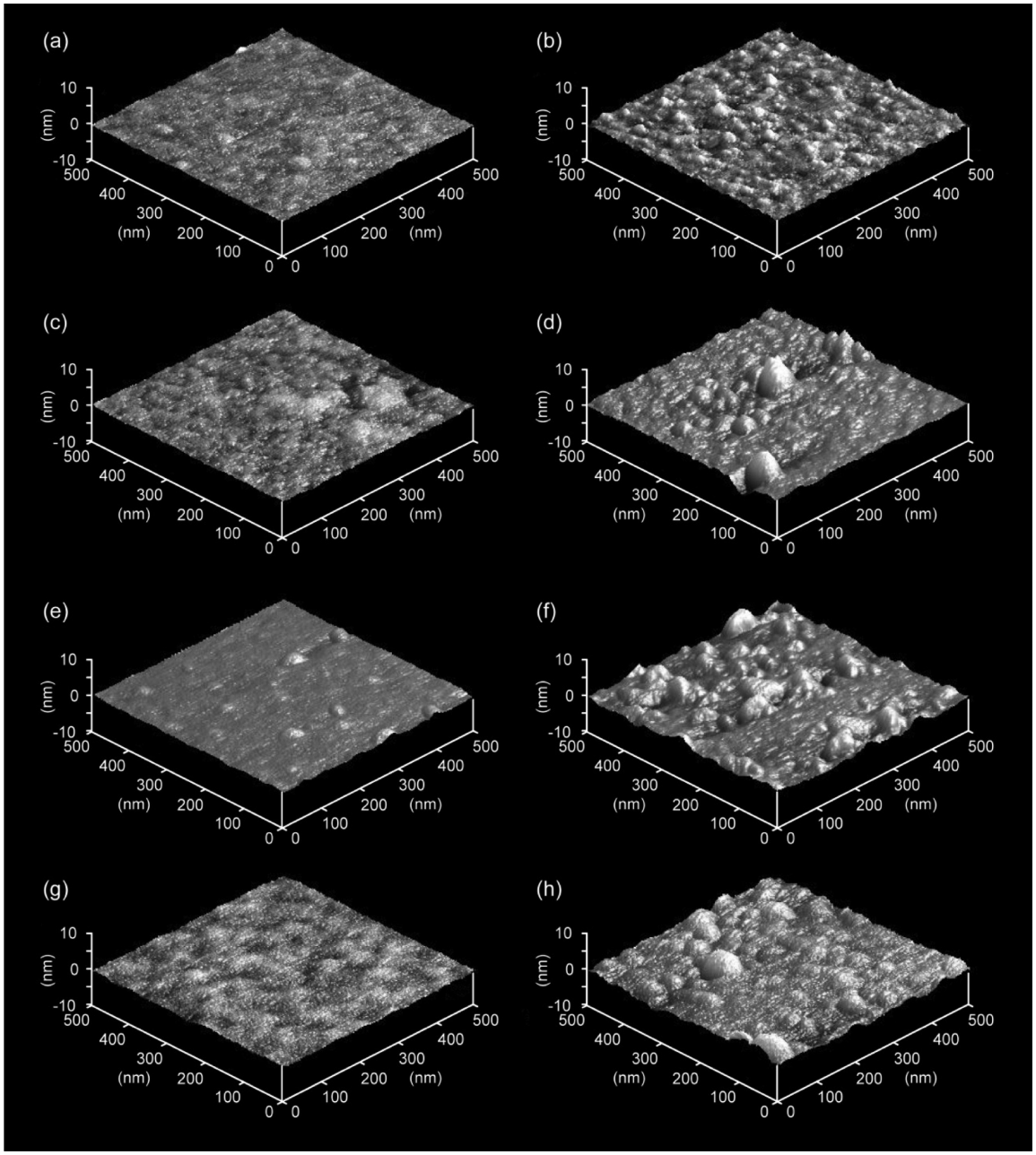

Figure 6. AFM images of (a) PSt-spin coated, (b) PSt-immobilized, (c) PAA-spin coated, (d) PAA-immobilized, (e) PNIPAm-spin coated, (f) PNIPAm-immobilized, (g) PMan-spin coated, and (h) PMan-immobilized silicon wafers. The surfaces of (a), (c), (e), and (g) were prepared by spin coating, and the surfaces of (b), (d), (f), and (h) were prepared by the maleimide-RAFT process.

and BSA on the PMan-immobilized glass slide were observed at 0.005 and 0.05 g/L, respectively. Con A (isoelectric point, pI: 4.5−5.5) and BSA (pI: 4.6) were bound with poly-L-lysine on the glass slide by electrostatic interactions, and there is no selectivity between anionic Con A and BSA. Thus, the specific interaction is dominant for selective detection of proteins over electrostatic interactions. The spots for FITC−BSA on the PMan-immobilized glass slide were darkened even at a high concentration range. The results suggest specific and strong binding between Con A and PMan. Immobilization of PMan on the glass slide enables the preparation of protein-recognizable biomaterials, i.e., protein microarrays.

Because PMan was tightly bound to Con A on glass slides, PMan-immobilized surfaces can be applied for micropatterning by photolithography. The micropattern formed on the PMan-immobilized glass slide by photolithography is shown in Figure 9. The distinct fluorescent pattern, which is identical to the microglid mesh design (Figure 9a), was visible on the PMan-immobilized surface (Figure 9b and c). The regions shaded by the microglid frame and mesh during photolithography became fluorescent, while the region exposed to UV through the microglid gap darkened. The surface brightness value was scanned linearly to determine the pattern geometry. I/I_0 on the dashed line in Figure 9b is shown in Figure 9d, where the change in I/I_0 on the mesh part (distance: 500−2500 μm) was determined. The I/I_0 value of the surface exposed during photolithography is approximately 1, suggesting that almost all of the amine groups, maleimide groups, and PMan on the UV-exposed surface have degraded. Spin coating is a facile technique to prepare thin polymer layers on surfaces. However,

dx.doi.org/10.1021/am301637q | ACS Appl. Mater. Interfaces 2012, 4, 5125−5133

Table 2. Roughness and Thickness of Polymer Layers on a Silicon Wafer Prepared by Spin Coating and the Maleimide-RAFT Process

polymer	RMS roughness (nm)[a]	thickness (nm)[b]
Spin Coating		
PSt	0.17	4
PAA	0.23	10
PNIPAm	0.22	11
PMan	0.25	14
Maleimide-RAFT Process		
PSt	0.34	15
PAA	0.80	5
PNIPAm	0.89	8
PMan	0.86	6

[a]RMS roughness on polymer layers was evaluated from AFM images. [b]Thickness of polymer layers was determined by ellipsometry.

Table 3. Amounts of Amine, Maleimide, and Thiol-Terminated Polymer Immobilized on the Surface of the QCM Cell

	immobilized amount[a]	
probe	(nmol/cm^2)	(ng/cm^2)
amine group	32.7	
maleimide group	4.3	
PSt		4210
PAA		627
PNIPAm		269
PMan		279

[a]The amounts of the functional groups and polymer on the QCM cell were estimated from the frequencies determined in the dry state.

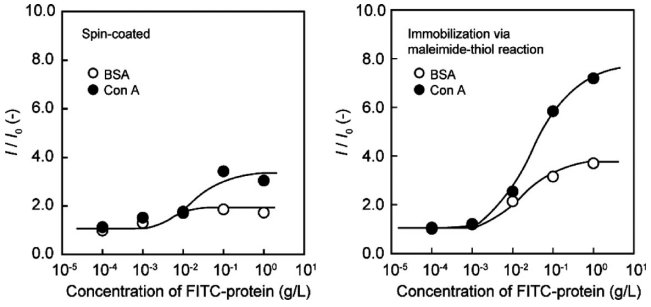

Figure 7. Relative fluorescent intensities of FITC–BSA and Con A on PMan-immobilized glass slides prepared by spin coating and the maleimide-RAFT process.

when water-soluble polymer-spin-coated surfaces are used in aqueous media, the polymer layer detaches from the surface due to weak interactions between the polymer and surface. As a result, the PMan-spin-coated glass slide is unsuitable for preparing protein microarrays (Figure 10). The sharply defined pattern of the microglid mesh design was not observed on the PMan-spin-coated surface. Photolithography and surface modification by the maleimide–thiol reaction on glass substrates could possibly be applied in bioanalytical devices such as protein–saccharide, antigen–antibody, and DNA microarrays.

4. CONCLUSION

In summary, a novel technique has been proposed for the immobilization of polymer on siliceous surfaces that is a

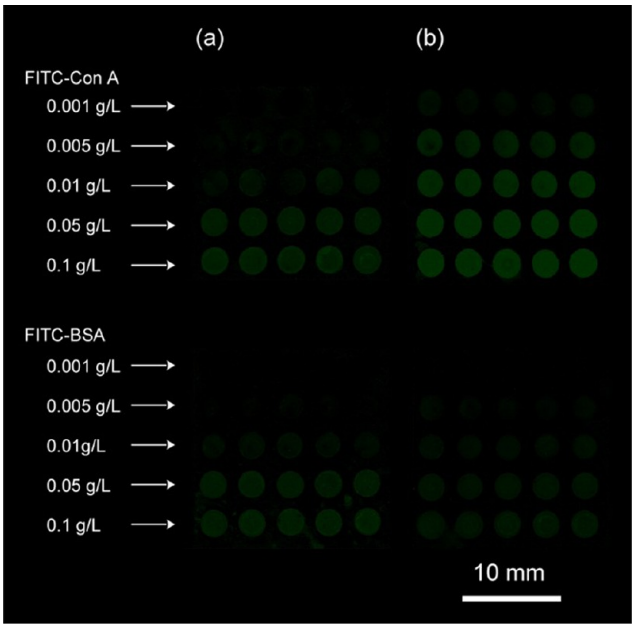

Figure 8. Fluorescent images of microarrays for the detection of Con A and BSA. (a) Commercially available glass slide coated with poly-L-lysine and (b) PMan-immobilized glass slide prepared by the maleimide-RAFT process.

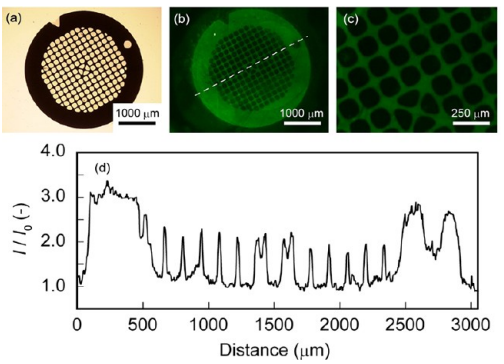

Figure 9. (a) Optical micrograph of the Cu grid used for photolithography, (b) and (c) fluorescent micrographs of FITC–Con A (10 mg/L) on the PMan-immobilized glass surface, micropatterned by photolithography, and (d) relative fluorescent intensity scanned on the dashed line in (b).

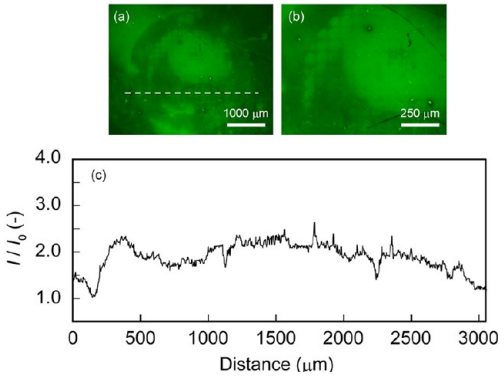

Figure 10. (a) and (b) Fluorescent micrographs of FITC–Con A (10 mg/L) on the PMan-spin-coated glass surface micropatterned by photolithography and (c) relative fluorescent intensity scanned on the dashed line in (a).

combination of maleimidation and RAFT polymerization. Amine layers were formed on the siliceous surface using an amine-containing silane coupling reagent, and then maleimidated surfaces were prepared by amide condensation with the aminated surface. When the polymers were immobilized on the maleimidated surface, smooth and thin polymer layers were formed, except for the hydrophobic polymer. The PMan-immobilized surfaces were used as platforms for protein microarrays and micropatterning by photolithography, where the interaction with Con A was more specific and stronger than on poly-L-lysine-coated and PMan-spin-coated glass slides. This technique could be used for surface modification of silicates, metal oxides, and cellulose using a variety of polymers.

■ ASSOCIATED CONTENT

Supporting Information

Details of the synthesis of the polymers via RAFT and free-radical polymerizations. This material is available free of charge via the Internet at http://pubs.acs.org.

■ AUTHOR INFORMATION

Corresponding Author

*Tel.: +81-92-802-2749. Fax: +81-92-802-2769. E-mail: miuray@chem-eng.kyushu-u.ac.jp.

Notes

The authors declare no competing financial interest.

■ ACKNOWLEDGMENTS

This work was supported by a Grant-in-Aid for Scientific Research on Innovative Areas (20106003 (YM) and 23106710 (TH)) and by a Grant-in-Aid for Young Scientists (B) (24760622 (HS)). We thank Prof. A. Takahara in Kyushu University for assistance with ellipsometry. We thank Dr. T. Ooba in Fukuoka Industrial Technology Center for lending the microarray scanner. We appreciate the helpful advice from Prof. Y. Iwasaki in Kansai University on photolithography.

■ REFERENCES

(1) Perrier, S.; Takolpuckdee, P. *J. Polym. Sci., Part A: Polym. Chem.* **2005**, *43*, 5347−5393.
(2) Moad, G.; Rizzardo, E.; Thang, S. H. *Aust. J. Chem.* **2005**, *58*, 379−410.
(3) Moad, G.; Rizzardo, E.; Thang, S. H. *Aust. J. Chem.* **2006**, *59*, 669−692.
(4) Roth, P. J.; Boyer, C.; Lowe, A. B.; Davis, T. P. *Macromol. Rapid Commun.* **2011**, *32*, 1123−1143.
(5) Bain, C. D.; Whitesides, G. M. *J. Am. Chem. Soc.* **1988**, *110*, 6560−6561.
(6) Bain, C. D.; Troughton, E. B.; Tao, Y. T.; Evall, J.; Whitesides, G. M.; Nuzzo, R. G. *J. Am. Chem. Soc.* **1989**, *111*, 321−335.
(7) Peaeson, G. R. *J. Am. Chem. Soc.* **1963**, *85*, 3533−3539.
(8) Senaratne, W.; Andruzzi, L.; Ober, C. K. *Biomacromolecules* **2005**, *6*, 2427−2448.
(9) Rusmini, F.; Zhong, Z.; Feijen, J. *Biomacromolecules* **2007**, *8*, 1775−1789.
(10) Lowe, A. B.; Sumerlin, B. S.; Donovan, M. S.; McCormick, C. L. *J. Am. Chem. Soc.* **2002**, *124*, 11562−11563.
(11) Sumerlin, B. S.; Lowe, A. B.; Stroud, P. A.; Zhang, P.; Urban, M. W.; McCormick, C. L. *Langmuir* **2003**, *19*, 5559−5562.
(12) Slavin, S.; Soeriyadi, A. H.; Voorhaar, L.; Whittaker, M. R.; Becer, C. R.; Boyer, C.; Davis, T. P.; Haddleton, D. M. *Soft Matter* **2012**, *8*, 118−128.
(13) Hoyle, C. E.; Lowe, A. B.; Bowman, C. N. *Chem. Soc. Rev.* **2010**, *39*, 1355−1387.
(14) Achatz, D. E.; Heiligtag, F. J.; Li, X.; Link, M.; Wolfbeis, O. S. *Sens. Actuators, B: Chem.* **2010**, *150*, 211−219.
(15) Dietrich, P. M.; Horlacher, T.; Gross, T.; Wirth, T.; Castelli, R.; Shard, A. G.; Alexander, M.; Seeberger, P. H.; Unger, W. E. S. *Surf. Interface Anal.* **2010**, *42*, 1188−1192.
(16) Chen, H.; Teramura, Y.; Iwata, H. *J. Controlled Release* **2011**, *150*, 229−234.
(17) Hasegawa, T.; Takeda, S.; Kawaguchi, A.; Umemura, J. *Langmuir* **1995**, *11*, 1236−1243.
(18) Ebara, Y.; Itakura, K.; Okahata, Y. *Langmuir* **1996**, *12*, 5165−5170.
(19) Allen, G. C.; Sorbello, F.; Altavilla, C.; Castorina, A.; Ciliberto, E. *Thin Solid Films* **2005**, *483*, 306−311.
(20) Wu, P.; Hogrebe, P.; Grainger, D. W. *Biosens. Bioelectron.* **2006**, *21*, 1252−1263.
(21) Weetall, H. H.; Hersh, S. L. *Biochim. Biophys. Acta, Enzymol.* **1969**, *185*, 464−465.
(22) Weetall, H. H. *Biochim. J.* **1970**, *177*, 257−261.
(23) Balachander, N.; Sukenik, N. C. *Langmuir* **1990**, *6*, 1621−1627.
(24) Pope, M. N.; Kulcinski, L. D.; Hardwick, A.; Chang, Y.-A. *Bioconjugate Chem.* **1993**, *4*, 166−171.
(25) Park, S. Y.; Ito, Y.; Imanishi, Y. *Macromolecules* **1998**, *31*, 2606−2610.
(26) Khademhosseini, A.; Jon, S.; Suh, Y. K.; Tran, T. T.-N.; Eng, G.; Yeh, J.; Seong, J.; Langer, R. *Adv. Mater.* **2003**, *15*, 1995−2000.
(27) Jon., S.; Seong, J.; Khademhosseini, A.; Tran, T. T.-N.; Laibinis, E. P.; Langer, R. *Langmuir* **2003**, *19*, 9989−9993.
(28) Grigoropoulou, G.; Stathi, P.; Karakassides, A. M.; Louloudi, M.; Deligiannakis, Y. *Colloids Surf., A* **2008**, *320*, 25−35.
(29) Wang, H.-J.; Zhou, W.-H.; Yin, X.-F.; Zhuang, Z.-X.; Yang, H.-H.; Wang, X.-R. *J. Am. Chem. Soc.* **2006**, *128*, 15954−15955.
(30) Jana, R. N.; Earhart, C.; Ying, Y. J. *Chem. Mater.* **2007**, *19*, 5074−5082.
(31) Kim, J. E.; Shin, H.-Y.; Park, S.; Sung, D.; Jon, S.; Sampathkumar, S.-G.; Yarema, J. K.; Choi, S.-Y.; Kim, K. *Chem. Commun.* **2008**, 3543−3545.
(32) Shah, S. S.; Howland, C. M.; Chen, L. J.; Silangcruz, J.; Verkhoturov, V. S.; Schweikert, A. E.; Parikh, N. A.; Revzin, A. *ACS Appl. Mater. Interfaces* **2009**, *1*, 2592−2601.
(33) SelegArd, L.; Khranovskyy, V.; Soderlind, F.; Vahlberg, C.; Ahren, M.; Kall, P.-O.; Yakimova, R.; Uvdal, K. *ACS Appl. Mater. Interfaces* **2010**, *2*, 2128−2135.
(34) Ritchie, C. M. S.; Bachas, G. L.; Olin, T.; Sikdar, K. S.; Bhattacharyya, D. *Langmuir* **1999**, *15*, 6346−6357.
(35) Abdelmouleh, M.; Boufi, S.; Salah, B. A.; Belgacem, N. M.; Gandini, A. *Langmuir* **2002**, *18*, 3203−3208.
(36) Hattori, K.; Hiwatari, M.; Iiyama, C.; Yoshimi, Y.; Kohori, F.; Sakai, K.; Piletsky, S. A. *J. Membr. Sci.* **2004**, *233*, 169−173.
(37) Li, S.; Zhang, S.; Wang, X. *Langmuir* **2008**, *24*, 5585−5590.
(38) Chauhan, A. K.; Aswal, D. K.; Koiry, S. P.; Gupta, S. K.; Yakjmi, J. V.; Suergers, C.; Guerin, D.; Lenfant, S.; Vuillaume, D. *Appl. Phys. A: Mater. Sci. Process.* **2008**, *90*, 581−589.
(39) Gebhardt, J. E.; Fuerstenau, D.W. *Colloids Surf.* **1983**, *7*, 221−231.
(40) Smith, E. A; Chen, W. *Langmuir* **2008**, *24*, 12405−12409.
(41) Miller, J. D.; Ishida, H. *Surf. Sci.* **1984**, *148*, 601−622.